Table 2

re	$\frac{d}{dt}\left(\frac{\rho}{P}\right)^{\frac{1}{3}}$ (h^{-1})	Q (kcal.mole^{-1})
	3·32 0·76	130 ± 6
	1·98 0·60	129 ± 5
	1·47 0·30	129 ± 5
	1·36 0·44	129 ± 5
	1·44 0·305	133 ± 6

certain whether tantalum would
tice, nor was the most satis-
g the alumina specimens known,
first attempt would be made by
s while in suspension in alcohol.
e was first ground with an alum-
e ground powder was then stirred
and allowed to settle for 10 min.
the oxide particles sufficiently
n, was then decanted, and the
permitting the alcohol to evapo-
of this selected oxide was then
owder whilst in suspension in
re containing 0·125% of tant-
rcentage was chosen so that the
of Ta_2O_5 in the alumina would
gO in the specimens containing

ree pairs of temperatures were
summarized in Table 3.

Table 3

re	$\frac{d}{dt}\left(\frac{\rho}{P}\right)^{\frac{1}{3}}$ (h^{-1})	Q (kcal.mole^{-1})
	2·15 0·27	147 ± 10
	2·0 0·34	145 ± 10
	2·64 0·52	154 ± 10

addition of tantalum pentoxide
ergy for diffusion to be increased
nole^{-1} for undoped alumina to
So marked a change in the dif-
en to confirm that the tantalum
e to enter the corundum lattice.

ON COEFFICIENTS

" diffusion coefficients may be
ranged form of Equation (6)

$$10^{-4}\,\frac{l^2kT}{\sigma\Omega_s}\,\frac{d}{dt}\left(\frac{\rho}{P}\right)^{\frac{1}{3}}$$

while the pre-exponential factor D_0 is given by

$$D_0 = D_M \exp(Q/RT)$$

The pore separation for one specimen of undoped alumina, i.e. that used during the determination of the factor Z (Section 3), was already known. Two further specimens, one doped with magnesia and the other with tantalum pentoxide, were examined microscopically by the methods described in Section 3, and were both found to possess pore separations of about 1 μm and grain sizes 1–2 μm. The two specimens were those referred to as 5 and 11 in Tables 2 and 3. For all three specimens, therefore, l was about 10^{-4} cm, while Ω_s (the volume of a complete "molecule" of alumina) was taken as being $4{\cdot}2.10^{-23}$cm^3 (calculated from the theoretical density of alumina and the atomic weights of the constituent ions). The values of D_M and D_0 could then be calculated: the results are shown in Table 4.

The three derived values of D_M are plotted on Figure 4, and through them are drawn lines (Plots A, B and C)

Table 4

Specimen	*Additive*	$\frac{d}{dt}\left(\frac{\rho}{P}\right)^{\frac{1}{3}}$ (h^{-1})	*Pressure* (dynes cm^{-2})	*Temperature* (°K)	D_M (cm^{2}sec^{-1}) (±70%)	D_0 (cm^{2}sec^{-1}) (±70%)
Z specimen	None	3·25	$3{\cdot}5\ 10^8$	1577	$4{\cdot}0\ 10^{-14}$	$3{\cdot}3\ 10^2$
5	MgO	3·32	$2{\cdot}8\ 10^8$	1577	$5{\cdot}1\ 10^{-14}$	$3{\cdot}8\ 10^4$
11	Ta_2O_5	2·0	$2{\cdot}1\ 10^8$	1655	$4{\cdot}3\ 10^{-14}$	$2{\cdot}7\ 10^6$

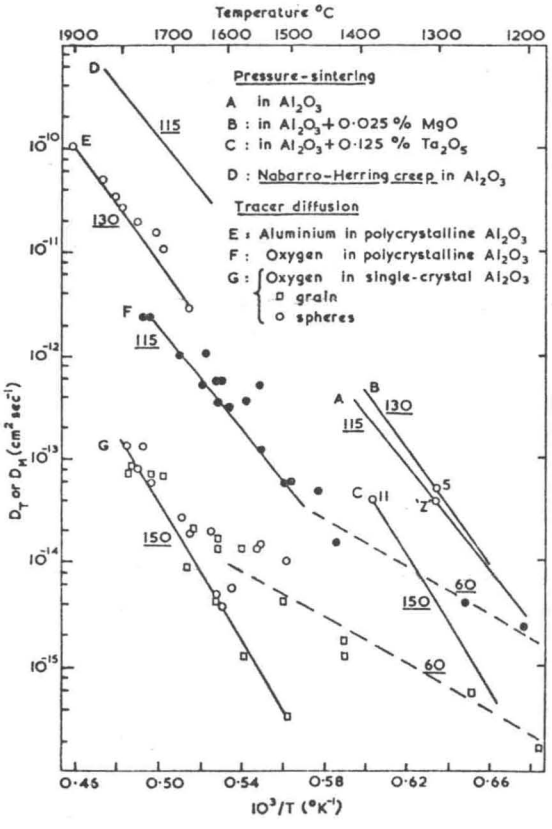

FIGURE 4
Diffusion coefficients in alumina.

with gradients appropriate to the activation energies measured for each type of specimen. The activation energy in kcal.mole^{-1} is shown underlined alongside each plot. Plots A, B and C thus represent the diffusion coefficients measured in all the present pressure-sintering experiments. Plot D on the same figure represents the diffusion coefficients (D_M) for Nabarro–Herring creep in polycrystalline alumina (sintered Linde A), recalculated from the results of HEWSON and KINGERY[5] using the modified Nabarro–Herring creep equation.

$$\dot{\epsilon} = \frac{40}{3}\,\frac{D_M\Omega_s\sigma}{L^2kT}$$

This plot falls very close to the extrapolation of plot A for pressure-sintering in alumina with no added impurity.

6. INTERPRETATION OF THE MEASURED ACTIVATION ENERGIES

The three activation energies determined in the present work (115, 130 and 150 kcal.mole^{-1} approximately) have all been quoted in the literature from time to time in connection with sintering or creep in alumina (Table 5).

Table 5

Experiment	*Activation energy* (kcal.mole^{-1})	*Reference*
Initial sintering (various aluminas)	142–150	JOHNSON and CUTLER[6]
Neck growth of spheres	131	KUCZYNSKI[7]
Grain growth	153	COBLE[8]
Sintering shrinkage	150	COBLE[8]
Sintering shrinkage	150	BRUCH[9]
Nabarro–Herring creep	~115	HEWSON and KINGERY[5]
Nabarro–Herring creep	~130	WARSHAW and NORTON[3]
Nabarro–Herring creep	~130	FOLWEILER[4]

In addition, PALADINO and KINGERY[10] measured an activation energy of 114 ± 15 kcal.mole^{-1} for aluminium tracer diffusion in polycrystalline alumina: and OISHI and KINGERY[11] observed three different activation energies for oxygen tracer diffusion in alumina: namely 110 ± 15 kcal.mole^{-1} with polycrystalline material, 152 ± 25 kcal.mole^{-1} with single crystals, and very approximately 60 kcal.mole^{-1} at lower temperatures with both types of sample. The experimental points for these tracer experiments are plotted in Figure 4.

Interpretation of the activation energy values measured in the present work, in terms of the published values for tracer diffusion, requires a theoretical analysis of the range of possible activation energies for diffusion observable in alumina.

6.1 The Theoretical Activation Energies for Ionic Diffusion in Alumina

The corundum lattice consists of oxygen ions arranged in nearly hexagonal close packing with aluminium ions filling two-thirds of the octahedral interstices. It is thus